UNIVERSIDADE DE SÃO PAULO
INSTITUTO DE GEOCIÊNCIAS

Petrochronology of anatectic rocks from Nazaré Paulista (SP), southern Socorro Guaxupé Nappe

ADRIANNA LUIZA VIRMOND

Dissertação apresentada ao Programa Geociências (Mineralogia e Petrologia) para obtenção do título de Mestre em Ciências

Área de concentração: Petrologia Ígnea e Metamórfica

Orientadora: Profa. Dra. Lucelene Martins

SÃO PAULO
2019

Serviço de Biblioteca e Documentação do IGc/USP
Ficha catalográfica gerada automaticamente com dados fornecidos pelo(a) autor(a)
via programa desenvolvido pela Seção Técnica de Informática do ICMC/USP

Bibliotecários responsáveis pela estrutura de catalogação da publicação:
Sonia Regina Yole Guerra - CRB-8/4208 I Anderson de Santana - CRB-8/6658

Virmond, Adrianna Luiza
Petrochronology of anatectic rocks from Nazaré Paulista (SP), southern Socorro Guaxupé Nappe / Adrianna Luiza Virmond; orientadora Lucelene Martins. -- São Paulo, 2019.
103 p.

Dissertação (Mestrado - Programa de Pós-Graduação em Mineralogia e Petrologia) -- Instituto de Geociências, Universidade de São Paulo, 2019.

1. petrocronology. 2. geochronology. 3. granite. 4. monazite. 5. zircon. I. Martins, Lucelene, orient. II. Título.

UNIVERSIDADE DE SÃO PAULO
INSTITUTO DE GEOCIÊNCIAS

Petrochronology of anatectic rocks from Nazaré Paulista (SP), southern Socorro Guaxupé Nappe

ADRIANNA LUIZA VIRMOND

Orientadora: Profa. Dra. Lucelene Martins

Dissertação de Mestrado

Nº 830

COMISSÃO JULGADORA

Dra. Lucelene Martins

Dra. Brenda Chung da Rocha

Dra. Mahyra Ferreira Tedeschi

SÃO PAULO
2019

“All that is gold does not glitter

Not all those who wander are lost;

The old that is strong does not wither

Deep roots are not reached by the frost”

(J. R. R. Tolkien)

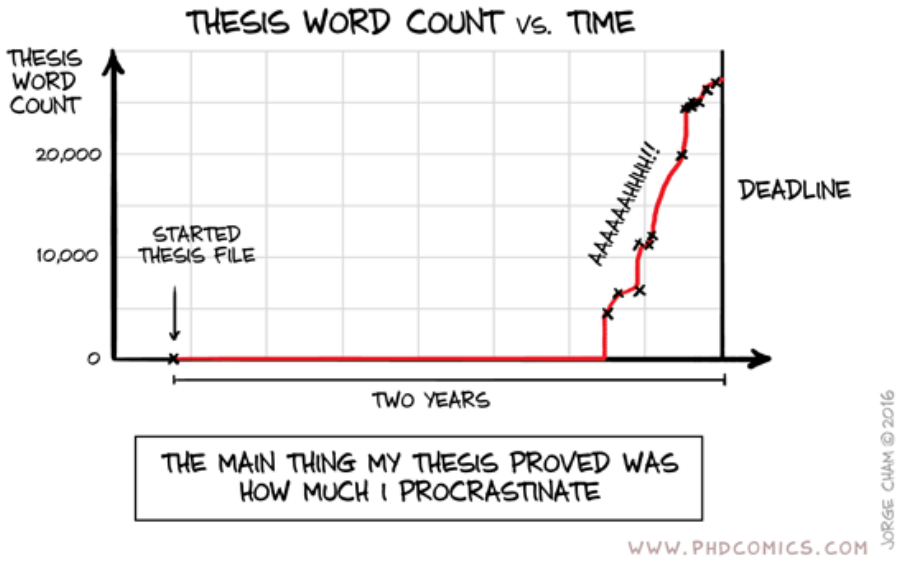

ACKNOWLEDGEMENTS

I would like to thank the Fundação de Amparo à Pesquisa do Estado de São Paulo – FAPESP (grant 15/01817-6) for funding and Coordenação de Aperfeiçoamento de Pessoal de Nível Superior (Capes) for the scholarship. I also would like to thank my supervisor, Lucelene Martins, for all the support during these years and for being a friend when I needed the most. Valdecir Janasi was also a great contributor who helped a lot along the way. To all lab technicians and IGc employees, you've helped me for 8 years now and I really appreciate it! Thanks!

I want to thank all my friends for the support during these years as grad student (in special my dear coffee buddies: Grega, Banana, Fofona, Rafa, Gari, Dana, Mocó's). We all had our phases along this *crazy roller coaster* that grad school is, and it was (and still is) great to look around and see familiar, friend faces willing to help. I also want to thank my friends from **Via Saber**. I could not have done it without your presence in my life!

Last, but not least, I want to thank my two families. The biological one, composed by the most amazing pair of women I'll ever have the pleasure to know: my mother and my sister. And also my dear friends, the family we choose to have besides us (to name a few: Erilio, Pringles, Exu, Gordelícia, Maia and cia) and my awesome housemates – my lovely *husband/wife* Sueca, our ***queen*** Banguela and our son, Belo. Thank you all for putting up with me all this time! I know *I* wasn't easy, I'm sorry. This dissertation is also your accomplishment.

Oh, of course, I also thank coffee for existing. Without you, my magic-black-divine fluid, none of these words would have left my mind into the paper.

RESUMO

Virmond, A. L., 2019, Petrocronologia das rochas anatéticas de Nazaré Paulista (SP), porção sul da Nappe Socorro Guaxupé [Dissertação de Mestrado], São Paulo, Instituto de Geociências, Universidade de São Paulo, 103 p.

Na porção sul da Nappe Socorro Guaxupé, interpretada como um arco magmático desenvolvido durante a amalgamação do Gondwana ocidental na orogenia Brasiliana Pan-africana, a região de Nazaré Pauslita é caracterizada pela ocorrência de afloramentos complexos de migmatitos e granitos anatéticos. Os granitos anatéticos ocorrem em duas variedades principais: granada-biotita granito cinza venulado (granito cinza) e granada leucogranito, que ocorrem como corpos isolados e como vênulas, em redes complexas cortando o granito cinza. Evidências em campo apontam para um possível *gap* de idade entre as variedades de granito, o qual investigamos nessa dissertação, usando geocronologia de zircão e monazita (por SHRIMP e LA-ICP-MS, respectivamente). A gênese dos leucogranitos também é investigada, usando química de elementos traço no zircão. As idades obtidas por SHRIMP para o granito cinza e vênula são equivalentes, dentro do erro – 626 ± 8 and 618 ± 8 Ma, respectivamente. Essas idades marcam aproximadamente o pico metamórfico e parte da evolução retrógrada da região. Idades de monazita confirma o gap entre idades de cristalização dos granitos: o granito cinza a ca. 621 ± 2 Ma, e leucogranitos, provavelmente em pulsos episódicos, entre 610 – 600 Ma. Conjuntos de zircão detrítico no migmatito variam entre 1100 e 2450Ma, indicando idade máxima de deposicão de 1100Ma para o protólito metasedimentar. Núcleos herdados de monazita registram idade de ca. 770 – 790 Ma, coincidentes com bordas de zircão com baixa razão Th/U. Os dados geocronológicos de zircão e monazita sugerem envento termal prolongado, registrando parte do evento progressivo, mas principalmente a trajetória retrógrada da região, num intervalo de aproximadamente 30 Ma. As idades herdadas de monazite, aliadas às bordas de zircão marcam um evento metamórfico em ca. 790 Ma, raramente reportado para a Nappe Socorro Guaxupé, mas coincidente com o metamorfismo do Complexo Apiaí-Embu (Sistema Orogênico Mantiqueira). Simulando composições de rocha parental a partir das composições de zircão tardio (sobrecrescimentos), observa-se que as composições modeladas são semelhantes àquelas analisadas na rocha, sugerindo equilíbrio entre as fases, e portanto, exclui-se a possibilidade de que hidrotermalismo teria modificado a composição dos grãos. Termometria de Ti em zircão e modelamento de granada e zircão sugerem evolução em sistema aberto para as rochas de Nazaré Paulista. Calculamos $D_{REE}^{zircon/garnet}$ e aplicamos o método proposto por Taylor et al. (2017). Núcleos de zircão estão em equilíbrio com granada interpretada como restito, enquanto sobrecrescimentos sçao compatíveis com granada peritética. Entretanto, para algumas variedades de leucogranito, zircão e granada não atingiram equilíbrio. Não se observa coerência no sistema isotópico Lu-Hf entre granito cinza e vênula, então, se o granito cinza é uma fonte para as vênulas, a participação de outra fonte é necessária para justificar a variação isotópica. O granada leucogranito apresenta evolução compatível com cristalização fracionada, enquanto o leucogranito com fibrolita provavelmente foi formado num sistema aberto. A evolução das rochas de Nazaré Paulista é mais complexa do que suposta previamente: um evento de anatexia ocorreu após o pico metamórfico, em ca. 630 – 625 Ma, originando o granito cinza; um segundo evento anatético, provavelmente envolvendo fusão por influxo de água do granito cinza, durante a descompressão, teria gerado, em pulsos, os leucogranitos, que se cristalizam entre 610 – 600 Ma.

Palavras-chave: geocronologia, petrocronologia, zircão, monazita, elementos traço, ETR, granito, migmatito

ABSTRACT

Virmond, A. L., 2019, Petrochronology of anatectic rocks from Nazaré Paulista (SP), southern Socorro Guaxupé Nappe [Master's Thesis], São Paulo, Instituto de Geociências, Universidade de São Paulo, 103 p.

In the southern portion of Socorro Guaxupé Nappe, interpreted as a magmatic arc developed during west Gondwana assembly in the Brasiliano-Pan-African Orogeny, Nazaré Paulista region is characterized by the occurrence of complex outcrops of migmatites and anatectic granites. The anatectic granites present two main types: a veined garnet-biotite granite (gray granite); and garnet leucogranites, that occur both as independent bodies, and as veins, forming complex networks cutting the gray granite. Field evidence points to an apparent crystallization gap between granite varieties, which we investigate in this dissertation, applying zircon and monazite geochronology (by SHRIMP and LA-ICP-MS, respectively). We also investigate the genesis of the leucogranites, using trace-element signatures of zircon and garnet. Obtained SHRIMP zircon ages for host gray granite and leucogranite veins are equivalent, within error - 626 ± 8 and 618 ± 8 Ma, respectively. These ages record near peak and part of the retrograde evolution of the region. Monazite LA-ICP-MS dating confirms the crystallization age gap between the granite varieties: the monazite from gray granite crystallized at ca. 621 ± 2 Ma, while monazite from leucogranites crystallized, probably in episodic pulses, between 610 – 600 Ma. Zircon inheritance sets in the migmatite vary from 1100 to 2450 Ma. Some inherited monazite cores from migmatite also yielded ages of ca. 770 – 790 Ma, coeval to very low Th/U zircon rims. Combined monazite and zircon geochronological data suggests a protracted thermal last event, recording part of the prograde and mostly the retrograde path of the region, during a time span longer than 30 Ma. Detrital zircon from the metatexite suggest a maximum deposition age of at least 1100 Ma, and a chemical signature of granitoid sources. The inherited zircon and monazite suggest a metamorphic event at ca. 790 Ma, rarely reported to Socorro Guaxupé Nappe, but coeval to the metamorphism registered by rocks in the Apiaí-Embu Terrane (Mantiqueira Orogenic System). Modelling bulk rock contents from zircon compositions, in late zircon phases, occurring as overgrowths, produce bulk rock compositions compatible empirical data, suggesting these phases were in equilibrium and no hydrothermal event modified these grains. Ti in zircon thermometry and zircon/garnet modelling suggest evolution in an open system for these rocks. We calculated $D_{REE}^{zircon/garnet}$ and applied the method proposed by Taylor et al. (2017). Zircon cores are close equilibrium with (what is interpreted as) restitic garnet and overgrowths are usually in equilibrium with late, peritectic garnet generation. However, for some varieties of leucogranite, zircon and garnet are never found to be in equilibrium. No coherence between Lu-Hf isotopy is found between the vein leucogranite and the gray granite, so, if the gray granite is a source for the veins, another source is necessary to account for isotopic variation. The garnet leucogranite present trends compatible with fractioned crystallization, while the fibrolite bearing leucogranite probably formed in an open system. Nazaré Paulista evolution is much more complex than previously thought: a primary anatexis event, after metamorphic peak, at around 630 – 625 Ma originated the gray granite; a second anatexis event, probably involving water-flux melting of the gray granite, during decompression, generated the leucogranites, which crystallized at 610 – 600 Ma.

Keywords: geochronology, petrochronology, zircon, monazite, trace elements, REE, granite, migmatite

TABLE OF CONTENTS

LIST OF FIGURES

LIST OF TABLES

1 INTRODUCTION

Timescales involved in granite genesis range from a few thousand to tens of millions of years, spanning at least seven orders of magnitude (Brown, 2013). Melting occurs during metamorphic cycles, which may take millions to tens of millions of years (Hermann and Rubatto, 2003), and a significant part of the evolution is above solidus, in the order of several million to tens of millions of years (Brown, 2013; Kriegsman and Nyström, 2003). Plutons take thousands to a few millions of years to form, by crystallization of several batches of melt (Brown, 2013, 2001), that, individually, can have residence times of more than 1 Ma (Kriegsman and Nystrom, 2003), under dynamic conditions with low melt percolation. For large amounts of anatectic melts, residence times vary from a few million to tens of millions of years (Brown, 2013; Rubatto *et al.*, 2009, 2001), although the numerical modeling of prograde heating of the deep crust suggests time scales of tens of millions of years are necessary to achieve ultra-high-temperature conditions (Clark *et al.*, 2011), and rocks maintain near-peak temperatures over extended periods of time (Kriegsman and Nyström, 2003; Thompson and England, 1984).

Since zircon and monazite can react during several processes (Taylor *et al.*, 2016) along the P – T – t path of a rock, their ages may span a long interval. The interpretation is that such an age spread is due either to a protracted tectono-thermal event, defining a long time span during which these minerals had conditions to form; or to multiple events during a single long-term event (e.g., multiple melting events, Rubatto *et al.*, 2009); or even different stages along the P – T – t path (e.g., Rubatto *et al.*, 2001; Rocha *et al.*, 2017).

The geochronology of accessory phases has substantially improved over the recent decades due to technical enhancements, such as the possibility of precisely dating spots of 20 – 30 µm, within a textural context (Engi, 2017; Kohn, 2016; Kylander-Clark, 2017; Taylor *et al.*, 2016; Williams *et al.*, 2017). Zircon and monazite are the main repositories for rare earth elements (REEs), Hf, Y, U and Th in igneous and metamorphic rocks. Even though they cannot be directly used in geochemical modeling (through equilibrium fractionation – Bea, 1996), REEs are useful petrogenetic tools (Whitehouse, 2003). Trace-element distribution in zircon may also be used in studies of provenance (Belousova *et al.*, 2002) and ore-forming processes (Nardi *et al.*, 2013). Hence, in recent years, many authors have called on all these features of

these minerals, building integrative models to understand the formation of rocks and their evolution over time (e.g. Hallett and Spear, 2015; Karmakar and Schenk, 2015; Martins *et al.*, 2009; B.C. Rocha *et al.*, 2017; Rocha *et al.*, 2018; Rubatto *et al.*, 2013).

Even though Nazaré Paulista anatectic rocks are well characterized in the literature (e.g. Janasi *et al.*, 2005; Martins *et al.*, 2009), the occurrence of spatially related migmatite and anatectic granites makes the region a good laboratory for studying crustal granite genesis, a potential poorly explored to date. In this dissertation, we explore petrochronological approaches to contribute to the understanding of evolution of Nazaré Paulista rocks, Socorro Guaxupé Nappe (NSG) and, to some extent, the generation of melts in the granitic crust.

1.1 Dissertation Structure

This dissertation was produced as two manuscripts. The first covers geochronological results for Nazaré Paulista anatectic rocks and contributes to the understanding of the metatexite inherited grains. The second manuscript focuses on zircon trace-element chemistry and how to apply it to constrain petrochronological processes in anatectic rocks. We also discuss possible mechanisms for the formation of the granites in Nazaré Paulista outcrops and their genetic relationship.

We start the dissertation by presenting a concise literature review, focusing mainly on petrochronology and how to use trace elements to constrain petrologic processes on anatectic rocks (chapter 2). We then introduce the methodology applied during the research (chapter 3). We present two manuscripts (chapters 4 and 5), with the proposed structures for them (except for methodology, which is all presented in chapter 3). We finish by presenting final remarks (chapter 6), addressing both articles. Figures and tables are numbered within each chapter, references for each draft are within the respective chapter; references for the other chapters are presented in the end (in chapter 7).

2 LITERATURE REVIEW

2.1 Petrochronology

All rocks are, to a certain extent, products of the transformation of previous rocks through time. Petrology and geochemistry show us these processes are often, somehow, preserved in the rocks. How and if this record will affect the age determination of a given rock is a matter of spatial and isotopic resolution (Engi *et al.*, 2017). Diverse stages of a rock evolution history can be recorded in the rock, especially in accessory phases (e.g., Catlos, 2013; Corfu, 2003; Hallett and Spear, 2015; Martins *et al.*, 2009; Rubatto, 2017). Hence, a rock does not have “one age”, but many different ages, which register different moments of its evolution; and only have complete meaning within the petrogenetic context it formed (Engi *et al.*, 2017). Defining this specific petrological context is one of the main objectives of Petrochronology, the new growing branch of geosciences.

Although petrochronology is a relatively new (and hyped) term - it was first used by Fraser *et al.* (1997), who concluded that the understanding of phase reaction history of a rock allows a more confident interpretation of zircon ages - the concern of correlating ages and textural domains in order to accurately interpret processes is been around for decades (e.g. Foster and Parrish, 2003; Rubatto, 2002; Vance *et al.*, 2003). The development (and enhancement) of high resolution in situ techniques, such as LA-ICP-MS and SHRIMP solves the sampling scale problem (analyzing major and accessory phases in too different scales makes it harder to correlate the minerals) (Kylander-Clark, 2017; Müller, 2003).

Profound knowledge of the studied area is critical when applying the petrochronological approach. The possible results of its application is, among others, determining exhumation rates (Rubatto and Hermann, 2001), subduction rates (Kaneko *et al.*, 2003), anatexis timing (Hallett and Spear, 2015; Rocha *et al.*, 2017), timing and deformation rates on shear zones (Muller, 2000), and magmatic chamber recharge processes (Schaltegger and Davies, 2017). Integrating all these data allow us, geologists, to better understand Earth tectonic evolution through time (Spear *et al.*, 2016; Kohn, 2016; Müller, 2003).

2.1.1 Petrochronological approaches

Petrochronology is, on a wider perspective, the incorporation of geochronometers in the petrologic and tectonic evolution of their host-rocks, characterizing geological and structural processes (Williams *et al.*, 2017). It means defining both relative and absolute time frames to metamorphic processes, quantifying t (*time*) on P-T-t and P-T-D-t paths (where P is pressure, T is temperature and D is deformation) (Müller, 2003; Spear *et al.*, 2016). Understanding the velocities and rates of geological processes allow us to comprehend tectonic mechanisms that drive crustal evolution (Spear *et al.*, 2016).

There are two main strategies to apply Petrochronology to metamorphic rocks: inferences from thermal-tectonic models; and pinning absolute ages in the P-T-t path (Spear *et al.*, 2016). The average velocity of the tectonic plates (about 10 cm/year) is known through detailed study of the seafloor spread velocities and is a reasonable upper limit for tectonic processes too. Even though thermal models do not, necessarily, determine the duration of the metamorphic crystallization and/or the exhumation processes, they provide a plausible timeframe where these processes happen. The pioneer models (*e.g.*, England and Thompson, 1984) calculated the time interval necessary to re-equilibrate the thermal disturbance caused by the (instantaneous) collision of two crustal segments, obtaining intervals on the order of tens of millions years, a period widely accepted by the scientific community as the duration of regional metamorphism (Spear *et al.*, 2016). However, petrochronology of metamorphic terrains shows this interval might have been overestimated (Spear *et al.*, 2016; Engi *et al.*, 2017). Spear *et al.* (2016) second approach involves the direct investigation of metamorphic rocks and may support and/or validate numeric models that simulate orogenesis and metamorphism (Vance *et al.*, 2003; Spear *et al.*, 2016). The authors suggest determining absolute and relative ages of many points (or segments) along the P-T-t path, either through diffusion studies (*e.g.*, geospeedometry) or geochronology.

The velocity of metamorphic processes can be obtained directly by system diffusion analysis (Spear *et al.*, 2016). Diffusion is temperature-dependent and happens faster at higher temperatures. One of the main techniques applying these inferences models diffusion in zoned garnets, a tool called Geospeedometry. This approach assumes that garnet is chemically homogeneous during metamorphic peak and that any chemical zoning and rim-core difference is generated via diffusive

exchanges within the mineral. Diffusion profiles and cooling rates can be calculated (e.g., Spear, 2004). These profiles, coupled with K-Ar and Ar-Ar ages and fission tracks ages allow a detailed description of the thermal history of metamorphic terrains during exhumation (Spear *et al.*, 2016).

Dating prograde metamorphism is tricky. Zircon and monazite, widely used geochronometers, have closing temperatures higher than ordinary metamorphic conditions and therefore are good candidates (Spear *et al.*, 2016). However, they often present chemical zoning, different age domains and inherited nuclei (e.g., Martins *et al.*, 2009; Rocha *et al.* 2017), which bring questions when interpreting the meaning of the obtained ages (Engi *et al.*, 2017).

Detailed imaging of internal features, either by cathodoluminescence (for zircon) or back-scattered electron (for zircon and monazite), allows researchers to choose which textures will be dated, improving the quality of interpretation. For monazite, X-ray compositional maps have also been used for textural characterization (e.g. Rocha *et al.*, 2017; Martins *et al.* 2009; Pyle and Spear, 2003). Many authors have described the different internal features found in both minerals (to be consulted – Zircon: Corfu *et al.*, 2003; Taylor *et al.*, 2016; Rubatto, 2017; Monazite: Catlos, 2013; Taylor *et al.*, 2016).

Under subsolidus conditions, these accessory phases may form by crystallization and solid-state reactions (Rubatto *et al.*, 2013); when melt is present, the saturation conditions of the liquid will control whether there is dissolution or precipitation. Since different events/reactions may lead to the precipitation or dissolution of accessory phases, internal zoning of these minerals might register different stages along the P-T path. Pyle and Spear (2003) observed four monazite generations, all related to different reactions for New Hampshire migmatites; Martins *et al.* (2009), working on Nazaré Paulista migmatite (SE Brazil), identified inherited nuclei (~795 Ma) and at least two different new generations of monazite: a ~635 Ma Y-rich phase, produced during progressive metamorphism; and ~610 Ma Y-poor overgrowths, interpreted to have precipitated from melt. Taylor *et al.* (2016) present a schematic P-T path showing the “expected” textural variation of garnet, zircon and monazite in a granulite facies terrain (Fig. 2-1).

Mineralogical Society of America has dedicated an edition to Petrochronology in 2017, where Engi *et al.* (2017) start by defining guidelines to apply it: first, one should choose a specific stage of evolution to be characterized (which involves determining the mineral phases, their compositions and textural relationships); once systematic

variations are identified (e.g., overgrowths, zoning, etc.), one should propose an isotopic system that can date the mineral/texture; if it is possible to correlate other petrogenetic parameters (in other words, determine P-T conditions to that specific texture) we go on to obtain ages.

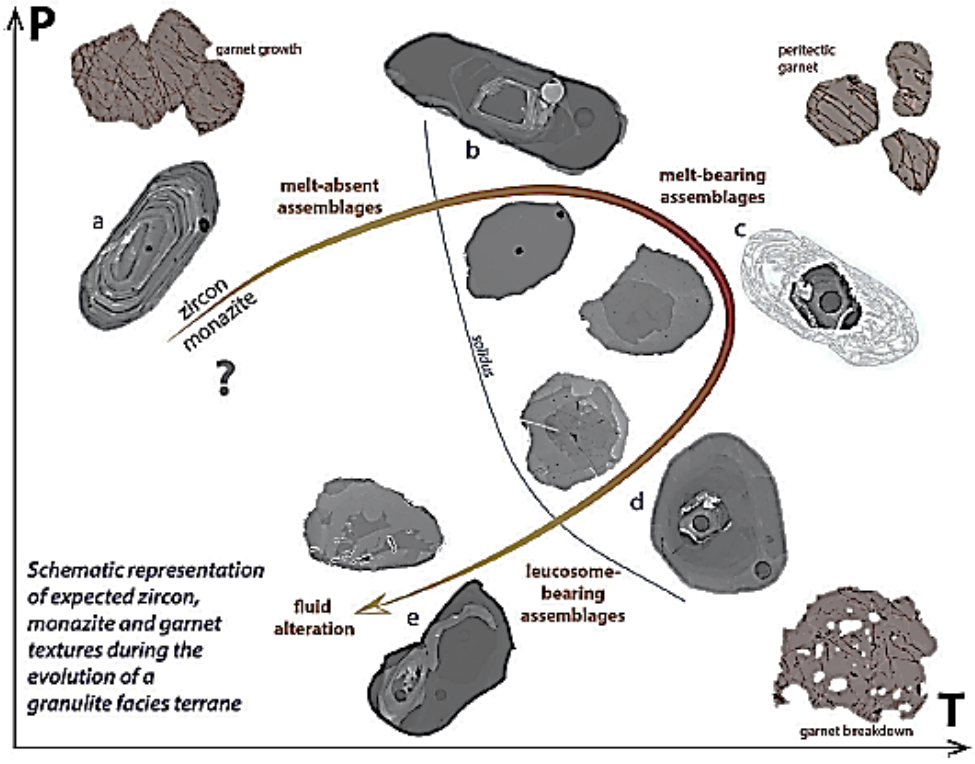

Figure 2-1 – Schematic representation of expected zircon, monazite and garnet textures during evolution of a granulite facies terrane. From Taylor *et al.* (2016)

The most important and challenging step is to determine accurately the petrogenetic conditions under which accessory phases formed. Although recent studies have made progress in determining the appearance and disappearance of these phases along the P-T path (e.g., Kohn *et al.*, 2015; Yakymchuk and Brown, 2014), accessory phase petrogenesis is still not well known. An alternative, widely applied, is correlating these phases to other major minerals, such as feldspar and garnet (e.g. Rocha *et al.*, 2017; Dumond *et al.*, 2015; Hallett and Spear, 2015). The correlation between accessory and major phases can be made based on textural relationships; modal and volumetric distribution; systematic compositional zoning; host-inclusion relationship; and, mainly, isotopic, major, minor and trace element distribution (Williams *et al.*, 2017, 2007).

2.1.2 Some limitations

Petrochronology is a brand new branch of geosciences, boosted by significant improvement on analytical techniques within the last few years (e.g., electron microprobe, LA-ICPMS and LASS -ICPMS, SIMS; Spear *et al.*, 2016; Baxter *et al.*, 2017; Engi *et al.*, 2017; Kylander-Clark, 2017; Williams *et al.*, 2017). Even though these advances have promoted better understanding of geological processes, some analytical limitations are yet to be overcame: insufficient spatial resolution (for example, for analyzing thin overgrowths, such as those presented in this work); low concentrations of elements in minerals, constantly below equipment detection limits; accuracy and precision of methods.

Spear *et al.* (2016) illustrate that, by dating a 500 Ma monazite with 1% uncertainty, we get an age of 500 ± 5 Ma. However, if a metamorphic event happened in a <5Ma interval, this methodology would not have enough temporal resolution to prove it. Yakymchuk *et al.* (2018) show that accessory phases can dissolve in time intervals from hundreds of thousands to a few million years, depending on the size of the crystal and the amount of water in the melt. Another promising branch within petrochronology is garnet. Baxter *et al.* (2017) consider it as “the ultimate petrochronometer”, but many improvements in garnet geochronology are still necessary to achieve that title.

There is room for improvement in chemical and textural characterization as well. Although X-ray compositional maps (obtained with electron microprobe) are quite advanced and widely used (especially for its petrochronological potential, (Lanari *et al.* 2018), they are mainly available for major elements. Engi *et al.* (2017) suggest that trace elements distribution maps would also be important to petrochronological studies. Raimondo *et al.* (2017) produced a REE compositional map of garnets (and added an extension to the software XMapsTools software, by Lanari *et al.* 2014), to assess the mobility of trace elements in this mineral. An important limitation of their approach is an analytical issue: because they were dealing with trace elements, imaging was possible by ablating a series of parallel rasters on LA-ICP-MS, which completely destroyed the analyzed grains.

One of the main obstacles for petrochronologists is understanding accessory phase paragenesis and incorporate them into phase equilibrium modeling (e.g., pseudosections, Yakymchuk and Brown, 2014). Even though many authors have been working with that, bringing substantial improvement to the field (e.g. Hallett and Spear,

2015; Kelsey *et al.*, 2008; Kelsey and Powell, 2011; Kohn *et al.*, 2015; Spear and Pyle, 2010; Yakymchuk *et al.*, 2018), many limitations are yet to be overcome.

Yakymchuk *et al.* (2018), for example, model the controls of Th/U ratios in metamorphic rocks, and present as limitations and/or assumptions: (i) assuming no kinetic barriers to the dissolution or crystallization of accessory minerals, even though these minerals can dissolve within 100 ka to 1 Ma (in a 6 wt% H_2O melt, Yakymchuk *et al.*, 2018 and references therein); (ii) only monazite and zircon are modeled, and no other accessory minerals are considered in the system (e.g., xenotime, allanite) which might also be important hosts for Th, U, REE, (Engi *et al.*, 2017); (iii) light REE, Zr, P are considered to not substitute into major rock-forming minerals, even though phases like garnet and feldspar might accommodate these elements and influence the stability of accessory phases (e.g., Bea, 1996, Fraser *et al.*, 1997); (iv) assuming Th substitution in accessory phases follows Henry's Law; (v) chemical and thermal equilibrium is achieved, so that all minerals are compositionally homogeneous, in equilibrium with each other and the melt; in natural rocks, most minerals, both major and accessory, preserve compositional zoning, and inclusions are chemically isolated from the matrix. Chemical zoning in accessory phases is actually a feature used to characterize different phases of the metamorphic history (e.g. Melo *et al.*, 2017; Engi, 2017; Rocha *et al.*, 2017; Rubatto and Hermann, 2007); (vi) apatite is considered to be unreactive in high P and low T (<660 ℃ at 8 kbar; <850 ℃ at 12 kbar) portion of modeling; and (vii) no adjustments to Ca in the metapelite model, to account for apatite, were made.

Taylor *et al.* (2016) state more experimental data are necessary to further improve nowadays petrochronology, for example on calculating REE partition coefficients between accessory and major phases and assessing mechanisms that control such distribution. Kirkland *et al.* (2015) come up with empirical equations (equations 1 and 2 in Kirkland *et al.*, 2015) relating the partitioning of Th and U between zircon and the whole rock and the temperature of zircon saturation. For example, Yakymchuk *et al.* (2018) use these equations to model the U and Th concentrations and Th/U ratios of zircon crystallized in equilibrium with anatectic melt. Kohn (2016) also suggests that improved thermodynamic modeling is necessary, regarding the understanding of REE diffusion mechanisms in metamorphic environs, which could be either "an obstacle or an opportunity" in petrochronology (Kohn and Penniston-Dorland, 2017). Engi (2017) reinforces that better pressure constraints are critical when dealing with thermobarometry of accessory phases, since thermal constraints

are well understood (many thermometers are based on accessory phases e.g., Ti in zircon, Zr in titanite, Zr in rutile, (Hayden *et al.*, 2008; Tomkins *et al.*, 2007; Watson *et al.*, 2006).

2.2 Zircon

Zircon is a zirconium orthosilicate mineral that occurs in many igneous and metamorphic rocks. Even though zircon has a simple chemical ideal composition, it is able to incorporate many chemical elements such as P, U, Th, Hf, Y, Sc, Nb and REE, in trace or minor proportion (Harley and Kelly, 2007; Hoskin and Schaltegger, 2003). These elements may occupy vacancies, or substitute Zr+4 or Si+4 in simple or coupled reactions (table 2-1). The ionic radius is the main factor controlling substitution: reactions that minimize tension effects on the crystal structure will be favored (Harley and Kelly, 2007).

Table 2-1 - Main chemical substitutions on zircon

		REACTION	*APPLICATIONS*
SIMPLE	(i)	$(U^{+4}, Th^{+4}) \leftrightarrow Zr^{+4}$	Geochronology (U-Pb system)
	(ii)	$Hf^{+4} \leftrightarrow Zr^{+4}$	Crustal evolution and magma sources (Lu-Hf)
	(iii)	$Ti^{+4} \leftrightarrow Zr^{+4}$	Thermometry Ti in zircon
COUPLED	(iv)	$(Y, ETR)^{+3} + P^{+5} \leftrightarrow Zr^{+4} + Si^{+4}$	Petrochronology Magmatic and metamorphic history Provenance
	(v)	$(Y, ETR)^{+3} + (Nb, Ta)^{+5} \leftrightarrow 2Zr^{+4}$	
	(vi)	$(Mg,Fe)^{+2}_{(int)} + 3(Y,ETR)^{+3} + P^{+5} \leftrightarrow 3Zr^{+4} + Si^{+4}$	
	(vii)	$(Al,Fe)^{+3}_{(int)} + 4(Y,ETR)^{+3} + P^{+5} \leftrightarrow 4Zr^{+4} + Si^{+4}$	

2.2.1 Internal features

Cathodoluminescence (CL) and back-scattered electron (BSE) images are used to characterize internal features of zircon. In CL, Dy^{+3} is the main elemental factor to control emission, and other elements such as Sm^{+3}, Eu^{+2} and Tb^{+3} are known to influence. However, the abundance of U^{+4} is the key factor geologists usually are concerned about – the presence of U and the defects caused by radiation decrease emission, hence creating dark zones (Corfu, 2003), constantly avoided for geochronological uses. In BSE images, the emission is a function of the average atomic weight of the scanned area. In general, zoning patterns are similar to those

produced by CL images, but dark zones in CL correspond to bright zones in BSE and vice versa (Corfu, 2003).

Zircon may present a wide variety of internal textures, depending on what process formed the mineral. For example, oscillatory zoning is known to be a magmatic feature. On metamorphic zircon, the texture may indicate the metamorphic facies in which the mineral formed. For detailed description and possible interpretations of these textures, see Corfu (2003) and Rubatto (2017).

2.2.2 U, Th and Th/U

U and Th are members of the actinide series and, due to their electronic configuration, have similar chemical properties, causing their geochemical coherence - this means these elements substitute each other in geological environments (Faure and Mensing, 2005). Since U is an incompatible element for most rock-forming minerals (Bea, 1996), it is incorporated in accessory phases, especially on Zircon (Hanchar and Westrenen, 2007). With ionic radius of 0.10 nm for U^{+4} and 0.105nm for Th^{+4}, these elements easily substitute Zr^{+4} (0.084 nm) in zircon structure, granting compositions of <5000 ppm of U and <1000 ppm of Th (Harley and Kelly, 2007). Zircon cannot accommodate Pb^{+2} in its structure during crystallization, due to the ionic radius of this element (0.129 nm). Hence, we assume all Pb found in zircon structure is a product of radioactive decay - a critical assumption that allows zircon geochronology (Harley and Kelly, 2007).

The Th/U ratio has been widely used to distinguish the origin of a zircon - either igneous, metamorphic or hydrothermal (e.g., Harley and Kelly, 2007; Harley *et al.*, 2007; Rubatto, 2017), probably because the data is obtained with the age (Rubatto, 2017). As a rule, crystals with Th/U < 0.1 are metamorphic (e.g., Rubatto, 2017) and ratios >0.1 are magmatic (unless crystals are weathered or hydrothermally altered - e.g., Belousova *et al.*, 2002; Harley and Kelly, 2007). However, Rubatto (2017) accepts there are exceptions to this rule, especially for rocks formed under ultra-high temperature conditions (>900 ℃, e.g., Möller *et al.*, 2003). Harley *et al.* (2007) believe Th/U ratio, when used alone, is not a reliable signature for metamorphic zircon. Therefore, we should consider other factors that influence Th and U distribution in a metamorphic rock.

It is consensus on the literature that the main factors that influence the incorporation of Th and U in zircon are: availability of these elements (metamorphic reactions, abundance in melt); and the partition of these elements between zircon and

other mineral phases, melt and fluids present (e.g., Harley *et al.*, 2007; Rubatto, 2017). If zircon crystallizes at the same time (or after) Th-rich phases (such as monazite and allanite), it will probably present low concentrations of Th and consequently very low Th/U ratios, as observed in metamorphic zircons from eclogite, amphibolite and granulite facies rocks with this paragenesis (Harley *et al.*, 2007; Rubatto, 2017). On the other hand, if zircon crystallizes without these phases, for example precipitating from a melt, it may present higher amounts of Th, and high to moderate Th/U ratios (Harley *et al.*, 2007). The same happens if the composition of the rock allows the crystallization of zircon in the absence of other competing phases (Rubatto, 2017).

Igneous petrology also applies Th/U ratio as a petrogenetic parameter, since the physical-chemical conditions of the magma, at the time zircon precipitates, will influence its Th/U ratios (e.g., Kirkland *et al.*, 2015). Igneous crystals usually present ratios ≥0.5 (Hoskin and Schaltegger, 2003), and inherited zircons (e.g., xenocrystals) are common, either because the magma temperature was not high enough to dissolve the inherited crystal; or because the system kinetics did not allow the dissolution (e.g., Bea *et al.*, 2007; Kirkland *et al.*, 2015).

Kirkland *et al.* (2015) discuss many factors that influence Th/U_{zircon} ratios in magmatic environments, including, among others: (i) parental magma composition; (ii) oxyanion UO_4^{-2} formation; (iii) relative competition for U and Th by different minerals; and (iv) crystallization speed. $Th/U_{whole\ rock}$ ratios (i) tend to increase SiO_2 contents, at the same time that Th/U_{zircon} ratio tends to decrease. The authors conclude that Th is more incompatible than U in zircon structure during magmatic crystallization, even when Th is more abundant on the rock; and that U^{+4} is more easily incorporated into zircon structure, as also suggested by Belousova *et al.* (2002). With UO_4^{-2} formation (ii), U becomes more mobile in aqueous solutions and might concentrate on hydrothermal fluids or melts, leaving a residue relatively enriched in Th (Kirkland *et al.*, 2015). Relative competition by U or Th in the magma (iii) occurs when mineral phases that can incorporate these elements crystallize at the same time. Low Th/U_{zircon} ratios may be formed when few minerals incorporate more U than zircon, or when mineral phases incorporate more Th than zircon (e.g., monazite, thorite). High ratios may be produced when mineral phases incorporate more U than zircon are present. Finally, the crystallization speed (iv) may affect Th/U_{zircon} ratios, reflecting if crystallization was under equilibrium conditions or not. Slow growth, under equilibrium conditions, for example in a deep chamber, will favor lower Th/U_{zircon} ratios, since the concentrations

of Th and U will be influenced only by the partition coefficients between zircon and melt (Kirkland *et al.*, 2015).

The authors propose a fractionation factor to, allying temperatures of zircon saturation and Ti in zircon thermometer, evaluate if there is a difference between the compositions of the rock and the liquid in equilibrium with the zircon. The fractionation factor is defined as $Th_{(zircon/rock)}/U_{(zircon/rock)}$ and, according to the authors, is more efficient than usual partition coefficients because it is not affected by fractional crystallization (which changes the liquid composition) and late crystallization of accessory phases, from differentiated liquids.

2.2.3 Hafnium

An important substitution that occurs in zircon is $Zr^{+4} \rightarrow Hf^{+4}$ (table 2-1) due to their similar ionic radius (0.084 and 0.083 nm, respectively); in addition, these elements have similar geochemical behavior in most systems in Earth (Claiborne *et al.*, 2006; Harley *et al.*, 2007). There is a complete solid solution with zircon ($ZrSiO_4$) and hafnon ($HfZrO_4$) as endmembers (Ramakrishnan *et al.*, 1969), but in natural crystals, due to elevated Zr/Hf ratios in nature (Claiborne *et al.*, 2006), Hf content in zircon usually varies between ~0.5 and 5 wt% (Belousova *et al.*, 2002; Hoskin and Schaltegger, 2003; Claiborne *et al.*, 2006). The occurrence of Hf-rich zircon is more common in evolved rocks, suggesting Hf abundance increases with magmatic differentiation (Hoskin and Schaltegger, 2003).

This substitution in zircon structure is particularly important because of the isotopic system Lu-Hf for crustal evolution studies, magmatic evolution, and sedimentary provenance (e.g., Westin *et al.*, 2016). Lutetium is a heavy REE, from the lanthanide series. It occurs in nature with two isotopes (^{175}Lu and ^{176}Lu), the latter being less abundant (~2.6%) and radioactive, producing ^{176}Hf.

In zircon, we use the isotopic system Lu-Hf, assuming that: (i) $^{176}Hf/^{177}Hf_{initial}$ varies very little throughout time, once $^{176}Lu/^{177}Hf$ ratio is commonly very low (<0.001), and therefore can be used to infer ages, in relation to a model (T_{DM}); (ii) the system remains closed for thermic events subsequent to crystallization of the mineral, since zircon closing temperature for Hf is elevated (ca. 1100 °C Cherniak *et al.*, 1997). Hence, $^{176}Hf/^{177}Hf$ ratio preserves a signature of the source where the crystal is formed. Fractionation of the Lu-Hf isotopic system occurs during mantle differentiation. With previously obtained U-Pb ages in zircon, we can use the $^{176}Hf/^{177}Hf$ ratio to calculate a

model age (T^{DM}_{Hf}) and εHf, parameters to infer the crustal evolution (time of residence, crustal formation), magma sources (juvenile mantle vs crustal reworking), and sedimentary provenance (Table 2.2).

Some authors use Zr/Hf as a petrogenetic tracer since the chondritic ratio of ~ 35-40 (Hoskin and Schaltegger, 2003; Claiborne *et al.*, 2006) varies little in crustal rocks. Because zircon is the main repository for Zr and Hf, and preferentially incorporates Zr, the crystallization of this mineral controls Zr/Hf ratios in coexisting magmas (Claiborne *et al.*, 2006): rocks with low Zr/Hf ratios are derived from evolved melts, extracted from sources with extensive zircon crystallization; zircons crystallized from these melts would present zones enriched in Hf, and therefore low Zr/Hf ratios. In Spirit Mountain batholith, studied by Claiborne *et al.* (2006), systematic variations on Zr/Hf rations, and in Hf and Ti contents - showing fluctuations in composition and temperature - suggest a >1 Ma history of repeated events of injection, fractionation and extraction of melt from a mush, resulting in a wide range of SiO_2 compositions observed in the rocks of the batholith.

Table 2-2 - Summary of Hf isotopy results and interpretations.

$^{176}Hf/^{177}Hf$	εHf	T_{DM}	Implications
High	+	T_{DM} close to the age of crystallization	Juvenile mantle input / few reworking
Low	-	T_{DM} much older than crystallization age	Longer crustal residence

2.2.4 Trace and Rare Earth Elements (REE)

Zircon is, along with monazite, an important REE, Y, U, and Th repository in igneous and metamorphic rocks, bearing up to 90 - 95% of REE of granitoid rocks (except for Eu; Bea, 1996). Especially in peraluminous systems, the fractionation of these phases controls partition of these elements between liquid and solid phases; other mineral phases have little influence, except for garnet (Bea, 1996). Accessory phases and its REE can be good petrogenetic tools (Whitehouse, 2003).

REE incorporation is dependent on pressure, temperature and bulk rock composition (Hanchar and van Westrenen, 2007). By understanding the distribution of these elements between magmas/melts and zircon, it is possible to reconstruct the conditions during crystallization of the mineral, and therefore the evolution of the rock

hosting it (e.g., Belousova *et al.*, 2002; Hanchar and van Westrenen, 2007; Chapman *et al.*, 2016).

Heavy REE (HREE; Ho to Lu) have ionic radius similar to Zr^{+4} in zircon structure, favoring substitution (see table 2-1); light REE (LREE; La to Nd) and middle REE (MREE; Sm to Dy), on the other hand, have much bigger radius, and therefore behave as incompatible elements for zircon (Hoskin and Schaltegger, 2003). Ce is the exception among LREE, reaching a few hundred ppm. Mantellic derived rocks present low REE + Y contents (<100 ppm) while crustal rocks present a few thousands ppm. In general, zircon presents less than 1 wt% REE+Y, and crystals presenting much higher values are suspects for altered grains or accidental analyze of inclusions (Hoskin and Schaltegger, 2003).

Most zircon populations present distinct intra and inter-grain compositional variation (Belousova *et al.*, 2006; Hoskin and Schaltegger, 2003 and references therein), reaching usually up to one order of magnitude. Whitehouse (2003) suggests disequilibrium crystallization, micro inclusion analyses, and even late opening of the system (especially for LREE) could explain significant variations in grains of the same sample.

Zircon REE abundance is reported in spider diagrams, normalized by the chondrite (e.g. C1 from McDonough and Sun, 1995) and plotted in $\log_{10}$ *vs* (La – Lu). LREE usually present abundances <10x chondrite while HREE present 10^3 to 10^4x. Unaltered magmatic zircon is enriched in HREE and depleted in LREE, with a steep distribution pattern and pronounced Ce positive and Eu negative anomalies (e.g., Hoskin and Ireland, 2000; Hoskin and Schaltegger, 2003; Whitehouse, 2003). The steep pattern is explained by the biased incorporation of HREE in spite of LREE, due to zircon structure. Mantle affinity crystals present no significant Eu anomaly and flatter HREE patterns (Hoskin and Schaltegger, 2003).

Ce and Eu anomalies are common to all igneous zircon. Ce anomalies are a function of oxygen fugacity in the system. In crustal, oxidant rocks, positive anomalies occur (Hoskin and Schaltegger, 2003). Europium anomaly may also be a function of oxygen fugacity. However, plagioclase fractionation before or during zircon crystallization seems to affect more the partition of this element (Hoskin and Schaltegger, 2003).

Belousova *et al.* (2002) proposes that the abundance of trace elements in zircon reflects the rock where it formed. The authors propose flow charts to distinguish source rock for zircons of uncertain origin (e.g. detrital grains), to be used with isotopic and

geochronologic data in sedimentary provenance studies. The flow charts use several elements (REE, Y, U, Hf, Sc, and others) and have varying success rates to accurately determine rock origin for zircons of known provenance. Hoskin and Schaltegger (2003), for example, criticize Belousova approach because there are metamitic crystals (altered by secondary processes and therefore not recording original conditions) in their database.

REE distribution between main and accessory phases are also important to constrain evolution of metamorphic rocks. Garnet is commonly the main repository of HREE in pelitic medium to high-grade metamorphic rocks. Therefore, zircon crystallizing during or after garnet growth, will present relatively flat, HREE distribution (in comparison to magmatic crystals; Rubatto, 2017). This feature is reported in the literature for eclogite and granulites (e.g., Rubatto, 2002; Rubatto *et al.*, 2006; Rocha *et al.*, 2017). According to Whitehouse (2003), distribution patterns for metamorphic zircon may vary a lot from igneous grains. Zircon is depleted in LREE when other REE-bearing accessory phases are LREE-rich (like monazite, titanite, and allanite; Rubatto *et al.*, 2006; Rubatto, 2017).

Europium negative anomalies are attributed to crystallization in presence of feldspar-bearing assembly (Rubatto, 2002; Rubatto, 2017). In eclogite facies rocks, zircon presents weak to absent Eu anomaly (Rubatto, 2017). In migmatite, anatexis reactions involving breakdown of mica, produces K-feldspar as peritectic phase, which may incorporate all Eu available. Hence, Eu anomalies in these rocks may be more pronounced regarding the protolith or a sub solidus equivalent (Rubatto *et al.* 2006; Rubatto *et al.*, 2013; Rubatto, 2017). HREE depleted zones have been attributed to growth of zircon in presence of garnet, directly linking the zone to the P-T trajectory of the rock (Whitehouse, 2003). However, determining the equilibrium between phases is not always simple, especially when both minerals are chemically zoned (Taylor *et al.*, 2017; Rubatto, 2017). Diffusive equilibrium may also play a difficulting role - Stepanov *et al.* (2016) shows that, above 700-900 °C, diffusive (re)equilibrium may occur in garnet, while zircon preserves growth stages along the metamorphism. Zircon also forms during cooling, by crystallization of melt (Rubatto, 2017), and present REE distribution similar to magmatic zircons (Hoskin and Schaltegger, 2003), although with more pronounced Eu anomalies (Rubatto, 2017).

Robust petrogenetic models for both igneous and metamorphic rocks can be drawn when allying REE distribution, textural context, internal features, Th/U ratios and

geochronology (e.g., Belousova *et al.*, 2006; Rocha *et al.*, 2017). This is one of the main focus of petrochronology.

Chapman *et al.* (2016) on the other hand, proposes a method to estimate parent rock trace element compositions using trace element composition from zircon. They empirically obtained a relationship between partition coefficients and REE concentration in zircon. We used this approach to compare the "expected" composition of parent rock to actual composition obtained by (Martins, 2005) and assess if secondary processes have affected the composition of our crystals.

Taylor *et al.* (2017) compared trends in REE partitioning between garnet and zircon coefficients for both experimental and empirical data. Their approach allows the use of all REE data from zircon, plotted against an average garnet composition. This average may be chosen according to petrochronological criteria, choosing, for example, rims and cores separately. In addition, their method allows analyses of any "mineral 1" plotted against "mineral 2", and can be used with other pairs of minerals, not only for garnet and zircon (Taylor *et al.*, 2017).

2.3 Monazite

Monazite is a REE orthophosphate - (REE)[PO_4] - but other elements are commonly incorporated in its structure as well, such as Th, U, Ca, Si, Y and Pb. Due to its monoclinic structure, incorporation of LREE is favored in monazite (Catlos, 2013; Engi, 2017; Williams *et al.*, 2017). Monazite presents a broad compositional range, possibly because its coordination site can deform and accommodate a great variety of cations (Th^{+4}, Y^{+3}, U^{+4}); this also may explain why monazite is stable under a broad interval of P-T conditions (Williams *et al.*, 2007; Catlos, 2013). Because of its structure, monazite does not incorporate high amounts Pb during crystallization of the mineral (Williams *et al.*, 2007; Engi, 2017). Nevertheless, accurate isotopic dating requires correction for the presence of this element (Williams *et al.*, 2007, 2017), depending on the dating method applied (*e.g.,* chemical dating does not require such correction, Montel et al.,1996).

Besides isomorphic substitutions ($REE^{+3} \leftrightarrow Y^{+3}$), two other mechanisms occur:

$$(1)\ 2\mathrm{REE}^{+3} \leftrightarrow Th^{+4} + Ca^{+2}$$

$$(2)\ \mathrm{REE}^{+3} + P^{+5} \leftrightarrow Th^{+4} + Si^{+4}$$

The first mechanism (1) is the solid solution with cheralite [$CaTh(PO_4)_2$] and is the most important in monazite; huttonite substitution ($ThSiO_4$), which also happens,

but in a smaller scale. In both mechanisms, U^{+4} can substitute for Th^{+4}. Monazite usually presents Th/U > 1, suggesting monazite tends to incorporate more Th (Williams *et al.*, 2007; Engi, 2017). Experimental data (Stepanov *et al.*, 2012) show huttonite substitution is favored under high pressure.

2.3.1 Internal Features

Monazite crystallized directly from the magma may present oscillatory zoning, reflecting the evolving composition of the liquid in equilibrium with the mineral. In addition, Th zoning and sector zoning, with selective adsorption of elements to the mineral surfaces, are common (Williams *et al.*, 2007; Catlos, 2013). Secondary processes, like fluid interaction and recrystallization, can alter primary zoning (Catlos, 2013). Metamorphic monazite, for instance, presents highly variable internal structures and composition.

Back-scattered-electron (BSE) images are often used to assess internal features of monazite and, even though many authors correlate different shades to Th content (e.g. Swain *et al.*, 2005), Catlos (2013) believes such correlation is not so simple. Compositional maps show the spatial distribution of key-elements, (like U, Th, Y, Ca, Pb) and indicate that chemical zoning may be correlated to the geological and geochemical history of the crystal (Williams *et al.*, 2007; Catlos, 2013; Taylor *et al.*, 2016).

2.3.2 Chemical composition and age interpretations

Monazite is one of the commonest accessory phases in low Ca peraluminous granites and occurs in rocks with composition varying from dioritic to evolved granites and pegmatites (Williams *et al.*, 2007). It is one the main repositories for REE and Th in igneous rocks (Williams *et al.*, 2017). In granitoids monazite presents high amounts of ThO_2 (3 - 5 wt%), a criterion often used to distinguish them from hydrothermal crystals (Catlos, 2013); however, there are exceptions, and Th zoning, with Th-poor cores and Th-rich rims, are common (Catlos, 2013).

Inherited monazite cores are reported in the literature, usually within distinct compositional zonings (e.g., Williams *et al.*, 2007). Chemical variability may help to understand the evolution of igneous systems, like pointing to magma mixing events (Dini *et al.*, 2004) and hydrothermal processes (Pettke *et al.*, 2005; Townsend *et al.*, 2001) including ore-forming events (Williams *et al.*, 2017).

Another key use of monazite is geochronology. Zircon and monazite are among the most applied geochronometers nowadays (Engi, 2017; Rubatto, 2017). Zircon is usually used for dating magmatic and metamorphic rocks, while monazite is more used to date high-grade metamorphism. For instance, monazite is the most applied geochronometer to constrain Himalayan metamorphism, due to the high reactivity of the mineral during Barrovian metamorphism (Rubatto *et al.*, 2013). During progressive metamorphism, under subsolidus, zircon is not very reactive and no newly formed zircon occurs; therefore, the mineral is not applied to these conditions.

Granitoid dating is dominantly obtained by zircon (Piechocka *et al.*, 2017). However, authors report difficulties in obtaining the age of leucocratic low-temperature granites, especially because of the high amount of inherited crystals these rocks bear (Bea *et al.*, 2007). Leucocratic granites are usually associated with intracontinental and collisional settings, derived from anatexis of crustal sources (<750 °C Ayres *et al.*, 1997), without mantellic input (Gao *et al.*, 2017). Low Zr solubility in low-temperature crustal magmas (<800 °C) limits the amount of zircon that can be dissolved and reprecipitated during crystallization of the rock (Piechocka *et al.*, 2017). Hence, Piechocka *et al.* (2017) show that monazite may record crystallization ages of "cold" granitic magmas more accurately than zircon.

Monazite is a common mineral in pelitic and psammitic metamorphic rocks, above greenschist facies. The mineral is unstable between diagenesis and the beginning of metamorphism, so the occurrence of monazite in these context points to detrital reliquiar origin (Spear and Pyle, 2002 and references therein). Monazite is widely used to date metamorphic rocks, especially high-grade (above greenschist) rocks (e.g., Rubatto *et al.*, 2001, 2006, 2013; Martins *et al.*, 2009; Catlos, 2013; Hallett and Spear, 2015; Rocha *et al.*, 2017). Different stages during the P-T trajectory can be recorded in compositional and age domains in monazite grains (Williams *et al.*, 2007; Kohn, 2016; Engi, 2017; Yakymchuk *et al.*, 2017). The mineral is more reactive during progressive metamorphism and can be formed under different P-T conditions, from solid state reactions, precipitated from fluids or crystallized from anatectic melts (Yakymchuk *et al.*, 2017).

Monazite-in reaction during progressive metamorphism is yet uncertain. Some authors believe it is allanite break-down at ~550°C (Williams *et al.*, 2007); others, defend it is garnet break-down, close to staurolite isograd (Yakymchuk *et al.*, 2017; Spear and Pyle, 2002). Crystals growing during progressive metamorphism often present chemical zoning, opposite to what happens to magmatic crystals, which

usually only presents Th-rich cores and Th-poor rims (Catlos, 2013). Kohn (2016) states that Th and Y contents decrease during solid-state reactions: Y decreases due to the growth of garnet; Th behavior is not well understood, but since monazite is the main repository of the element in metamorphic rocks, any newly formed crystals will be Th-poor because of earlier crystallized monazite. The role of apatite break-down in supra-solidus rocks is uncertain (Yakymchuk *et al.*, 2017). However, subsolidus apatite breakdown has been associated with monazite formation in some contexts (e.g., Rocha *et al.*, 2017).

In anatectic rocks, chemical variability patterns are different. During anatexis, it is common that monazite dissolves, since it becomes unstable (Kohn, 2016; Spear and Pyle, 2002). Dissolution is favored by increasing the amount of water and decreasing pressure in the melt (Stepanov *et al.*, 2012). Because of these factors, monazite crystals that record metamorphic peak are not expected. During cooling and crystallization, a new Th and Y-rich monazite forms around reliquiar cores (Kohn, 2016). According to Kohn (2016), this systematic variation allows us to identify the origin of the monazite during the P-T trajectory:

- Old, possibly inherited cores - present ↑Y and ↑Th, usually on cores;
- Crystals formed during progressive metamorphism, by solid-state reactions, in the presence of garnet - present ↑Th and ↓Y, formed <700°C.
- Post-anatexis crystals, crystallized from the melt - ↑Y and ↑Th, usually as overgrowths.

3 METHODOLOGY

We analyzed zircon and monazite mineral separates from the four main varieties of Nazaré Paulista granites - grey granite (NP74C); vein leucogranite (NP74D); sillimanite-bearing leucogranite (NP74AD) and garnet leucogranite (NP74U) – and Nazaré Paulista migmatite, associated with them (NP74AB). The preparation of the concentrates followed the standard procedure from CPGeo (Geochronology Research Center), Universidade de São Paulo.

3.1 Imaging

We obtained cathodoluminescence (CL) and backscattered electron (BSE) images of the crystals for zircon and monazite, respectively. Zircon CL images were obtained at SEM Laboratory, GEOLAB (High-Resolution Geochronology Laboratory), Universidade de São Paulo (USP), using a FEI Quanta 250 Scanning Electron Microscope (SEM) and XMAX CL detector (Oxford Instruments), using 5μm wide beam; HV of 15 kV; working distance of 17mm and magnification of 170x. Monazite BSE images were obtained on the SEM at LCT (Laboratório de Caracterização Tecnológica), Universidade de São Paulo. Their equipment is a Quanta FEG 650, with EDS Bruker (software espirit 1.9) system and a Quantax 400 detector, working with a 5.5 μm wide beam; HV of 20 kV; working distance of 14mm and magnification of 100x, in a high vacuum system.

BSE images of zircon from the migmatite (**NP74AB**; mesosome portion only) were also obtained at LCT, working with 6 μm wide beam; HV of 30 kV; working distance of 14 mm and magnification varying between 1500 and 11500x, depending on the size of the crystal. Monazite images were digitally modified to improve visualization of internal features using CorelDraw X8 image editing package.

3.2 Geochronology

We obtained zircon SHRIMP ages for two of the samples - the grey granite (**NP74C**) and the leucogranite (**NP74D**) that occurs as veins on it - at GEOLAB, Universidade de São Paulo, using 24 μm spots and the laboratory analytical procedures, as described in Sato *et al.* (2014). The zircons from the migmatite (only mesosome portion) and all of the monazite isotopic ages were obtained at GPGeo,

Universidade de São Paulo, using a Neptune multi-collector ICP-MS, coupled to a 193 nm Excimer Laser. We used spot sizes of 25 μm and repetition rate of 6 Hz.

3.3 Statistical treatment of geochronological data

Spencer *et al.* (2016)suggest a flow chart to improve statistical robustness of U-Pb zircon geochronology data treatment (and therefore, its interpretations). The same strategy was applied to both U-Pb zircon and monazite U-Pb isotopic ages presented here. Even though Spencer *et al.* (2016) do not, necessarily, present new approaches, they summarize already applied tools. Here, we present some of their more important discussions and suggestions.

- *Discordance* – expresses the difference between ages measured through different isotopic systems, and reflects, qualitatively, if the isotopic systems of the mineral were preserved after crystallization (Spencer *et al.*, 2016 and references therein). The most used value is ±10%. Spencer *et al.* (2016) suggest plotting the ages obtained for two different systems (with their error ellipses) and discard the analyses that do not lie on the 1:1 line (unless the discordant data defines a Discordia curve).
- *"Best age"* - Spencer *et al.* (2016) suggest adopting 1,5Ga as a turning point: for younger crystals, use $^{206}Pb/^{238}U$; while for older crystals, use $^{207}Pb/^{206}Pb$. When the average fits the Concordia (within its analytical error), the authors suggest using ConcAge, since optimizes both $^{206}Pb/^{238}U$ and $^{207}Pb/^{206}Pb$ ages.
- *MSWD* – The mean square weighted deviation (MSWD) is a parameter that evaluates to what extent the weighted average and uncertainty represent a single population of grains. An MSWD = 1 means the observed data and weighted average do not under- nor overestimate the associated uncertainties. Higher values mean the uncertainties were underestimated, or that the data spread is natural; smaller values suggest an overestimation of uncertainties, or that the weighted average does not represent the real spread of the sample. In addition, based on the metrics of Wendt and Carl (1991), Spencer *et al.* (2016) suggest a way of defining an "acceptable" range for MSWD values, based on the amount n of data collected: MSWD ± $1+2\sqrt{2/f}$ (where f=n-1).

3.4 Lu-Hf isotopic analyses

Analyses of Lu and Hf isotopic ratios in zircon were performed at CPGeo, University of São Paulo, on the samples previously dated by SHRIMP. We used a Neptune multi-collector ICP-MS, coupled to a 193nm Excimer Laser, with a 47μm spot size beam, laser fluency of ~8.55 J/cm² and repetition rate of 7 Hz. GJ-1 zircon standard (Jackson et al., 2004) was used for calibration.

3.5 Trace element analyses

Zircon trace element analyses were performed at NAP Geoanalítica Laboratory, Universidade de São Paulo, using a Thermo Scientific iCAP Q ICP-MS coupled to a New Wave UP 213 nm laser ablation system. We used 25μm wide and 60μm long rasters to analyze different chemical zones (most of which are also dated) within the grains. Laser fluency is 14 Jcm-2, with repetition rates of 20 Hz and pace velocity of 1 μms-1. The methodology follows what Andrade *et al.* (2014) propose. NIST-610 (Pearce *et al.*, 1997) as used as an external standard, while NIST-612 (Pearce *et al.*, 1997) and zircon zr91500 (Wiedenbeck *et al.*, 2004) were used as reference materials. Data reduction was performed on the software Glitter (Van Achterberg *et al.*, 2001), with careful selection and exclusion of potential inclusions (such as P, Ca, Th, K, Ti, Y outliers, Zhong *et al.*, 2018).

Following an approach widely used in literature (e.g., Belousova *et al.*, 2006), stoichiometric Zr for zircon (67%) was used as internal standardization. We performed EPMA analyses on some crystals to evaluate if the stoichiometric approach was adequate as the internal standard. Using these values as new parameters in Glitter, the difference of critical elements was never more than 3% and always within the analytical error. Hence, we adopted the stoichiometric value for all analyses. Table 3-2 presents zr91500 REE contents (in ppm) obtained, compared to that reported on literature.

REE and Y data from garnet were compiled from an unpublished thesis (Martins, 2005). According to this author, data were determined via laser ablation inductively coupled plasma mass spectrometer (LA-ICP-MS) on the Boston University using a VG Elemental PQ Excel and Merchantek/VG 213 nm Nd-YAG laser. Garnet were ablated using a 10 Hz repeat rate and 50 μm spot size, and the estimated detection limits and precision were 10 ppb and 1–2%, respectively. Time-resolved data consisted of 60 s measurements of the gas blank followed by 60 s of the sample signal. NIST SRM-610

glass was used as the external standard, and Ca (from electron microprobe analysis) as the internal standard.

Table 3-1 - REE concentrations for zr91500, used as reference material Values are reported for both our analyses and GEOREM (Jochum *et al.*, 2005).

	This work		GEOREM			This work		GEOREM	
	Avg	**STDEV**	**Avg**	**STDEV**		**Avg**	**STDEV**	**Avg**	**STDEV**
P	28.0	7.3	24	1	**Dy**	9.0	1.2	12	1
Y	116	5.2	140	14	**Ho**	3.9	0.3	4.8	0.4
Nb	0.9	0.2	0.79	0.07	**Er**	19.9	1.1	25	3
La	0.1	0.0	0.006	0.003	**Tm**	5.1	0.4	6.9	0.4
Ce	2.3	0.3	2.6	0.3	**Yb**	55.6	2.7	74	4
Pr	0.1	0.0	0.024	0.015	**Lu**	10.9	1.0	13	1
Nd	0.8	0.1	0.24	0.04	**Hf**	5718	275	5900	300
Sm	0.7	0.1	0.5	0.08	**Ta**	0.5	0.1	0.5	0.1
Eu	0.3	0.1	0.24	0.03	**Pb**	61.3	23.4	15	2
Gd	1.5	0.3	2.2	0.3	**Th**	23.0	1.3	30	3
Tb	0.7	0.1	0.86	0.07	**U**	69.2	2.1	80	8

Avg = average; STDEV = standard deviation

3.5.1 Filtering of zircon trace element

The standard routine in the laboratory uses rasters (instead of spots) to analyze zircon for trace elements (see Andrade *et al.*, 2014). Therefore, we took advantage of this technique to analyze thin overgrowths we could not date, by drawing lines within zones. The main advantage of using raster is the shallower ablated pit, so mixture of different zones in 3D level is minimized. When the mixture of two zones was inevitable (usually due to the thickness of the overgrowth), we separated the signal using Glitter software, combining both time of analyses (e.g., 20 first seconds correspond to zone A), change in proportion of elements and REE distribution patterns.

Because of the highly variable composition we found in our zircon, and aiming to accurately interpret the data, we created a routine to filter the data based on trace element geochemistry. We selected sensible elements to help monitor the presence of inclusions: Ca, P, Y, Ti and Th, for apatite, xenotime, monazite and titanite, respectively (as suggested by Zhong *et al.*, 2018). Compiling nearly 50000 data available of zircon on GEOROC, selecting granitoid rock types, we calculated the average contents of these elements in zircon and applied a 2x standard deviation range buffer around the

mean of the distributed data. Hence, we defined an upper limit of composition of commonly occurring zircon, for each sensible element, and applied this filter to our data (Table 3.3). Any “zircon” with higher contents of these elements is, therefore, considered contaminated, and the analysis was discarded. We also discarded outliers that did not necessarily fit the first cut, but that yet present much higher values.

The filtering process we applied mitigate the possibility of contamination by microscopic and nanoscopic inclusions.

Table 3-2 - Filtering of data - values adopted as upper limits

Element	Mean (ppm)	StanDev (ppm)	Upper Limit (ppm)
Ca	1466.76	3013.12	7493.00
P	1054.20	2005.03	5064.26
Th	430.82	2578.26	5587.35
Ti	27.45	238.33	504.12
Y	2374.34	5089.32	12552.98

6 FINAL REMARKS

The gray granite is older than the leucogranites, and its garnet and zircon trace element composition evoke entrainment of restite, as previously suggested by Martins (2005). In addition, the inheritances set suggest a source different for the vein leucogranite and the metatexite, and isotopic (Lu-Hf) information suggest another source is involved to produce the vein leucogranite. The age of the gray granite is compatible with magmatic crystallization, right after the main metamorphic event of the nappe (ca. 635 Ma, Rocha *et al.*, 2017; Mora *et al.*, 2014, Martins *et al.*, 2009; Basei *et al.*, 1995). This age is also reported for monazite cores (Martins *et al.*, 2009). Many authors indicate that crystallization of zircon and monazite occurs mainly during the retrograde path (e.g. Hallett and Spear, 2015; Kelsey *et al.*, 2008; Kelsey and Powell, 2011; Taylor *et al.*, 2016; Yakymchuk, 2017).

The geochronological coherence between monazites from leucogranites, metatexite and leucosome (Martins *et al.*, 2009) suggests they could have formed during the same thermal event. Field evidence and the presence of andalusite both in the vein leucogranite and the metatexite, suggests decompression to shallower portions of the crust. Hence, our data suggest two granite events (gray granite formation at ~625 Ma and leucogranites at ~608 Ma), during a single protracted thermal event, spanning at least 30 Ma (near peak and retrograde paths). Other authors have suggested such long-term event for the nappe as well (e.g. Rocha *et al.*, 2017; Mora *et al.*, 2014; Tedeschi *et al.*, 2018). The metatexite record Meso and Paleoproterozoic detrital zircon cores in sets different than those from the gray granite. The vein leucogranite presents detrital Neoproterozoic cores, while the metatexite records these ages on low Th/U metamorphic overgrowths. This age may represent a metamorphic event, rarely reported to Socorro Guaxupé Nappe, but described in the Apiaí-Embu Terrane (Mantiqueira Orogenic System), record of the amalgamation of Western Gondwana (Campanha et al., 2019).

Martins (2005) offered two possibilities for the formation of the vein leucogranite: it corresponds to fractionated remobilized melt, representing final liquids from the gray granite itself; or it was formed by remelting of the mush, during decompression.

In Nazaré Paulista, the boundaries between the gray granite and its leucogranite veins are diffuse and do not present selvedges; the spatial disposition of the veins is variable, with both structurally controlled sites and no control at all. These field evidences and the spread of zircon ages are compatible with a remelting, water-

induced hypothesis to the vein formation, if we compare the gray granite and the vein leucogranite as a single system. On the other hand, the different sets of zircon inheritances found on the gray granite and the vein leucogranite, might indicate another source mixing with the gray granite to form the veins. Because the set of inheritances of the leucogranite is, at least, partially coherent with the metatexite, we believe they could be genetic linked. Further work is necessary, regarding whole rock and mineral and isotope geochemistry, to constrain how this system could have evolved.

The garnet leucogranite (NP74U) seems to have evolved in a closed system: zircon composition variation (decreasing Th/U and Zr/Hf) and garnet-zircon modelling are compatible with an evolving system, without external inputs. The fibrolite bearing leucogranite probably evolved in a different, particular manner. No equilibrium between garnets and zircon is observed in the sample, even though it has a composition compatible with fractionation from the gray granite. The spread of compositions should indicate an open system to this leucogranite variety as well.

Allying all geochronological data presented here and the modelling to check possible mechanisms for formation, we obtain a model for the evolution of Nazaré Paulista rocks: a primary anatexis event, at around 630 – 625 Ma originated the gray granite; and a second event, probably involving water-flux melting of the gray granite generated the leucogranites, which crystallized at 610 – 600 Ma.

7 REFERENCES

Andrade, S., Ulbrich, H.H., de Barros Gomes, C., Martins, L., 2014. Methodology for the Determination of Trace and Minor Elements in Minerals and Fused Rock Glasses with Laser Ablation Associated with Quadrupole Inductively Coupled Plasma Mass Spectrometry (LA-Q-ICPMS). Am. J. Anal. Chem. 05, 701–721. https://doi.org/10.4236/ajac.2014.511079.

Ayres, M., Harris, N., Vance, D., 1997. Possible constraints on anatectic melt residence times from accessory mineral dissolution rates: an example from Himalayan leucogranites. Mineral. Mag. 61, 29–36. https://doi.org/10.1180/minmag.1997.061.404.04

Basei, M.A.S., Siga Jr., O., Sato, K., Sproesser, W.M., 1995. A metodologia Urânio-Chumbo na Universidade de São Paulo: Princípios, aplicações e resultados obtidos. An. Acad. Bras. Cienc. 67, 221–237.

Baxter, E.F.F., Caddick, M.J.J., Dragovic, B., 2017. Garnet: A Rock-Forming Mineral Petrochronometer. Rev. Mineral. Geochemistry 83, 469–533. https://doi.org/10.2138/rmg.2017.83.15

Bea, F., 1996. Residence of REE, Y, Th and U in Granites and Crustal Protoliths; Implications for the Chemistry of Crustal Melts. J. Petrol. 37, 521–552. https://doi.org/10.1093/petrology/37.3.521

Bea, F., Montero, P., González-Lodeiro, F., Talavera, C., 2007. Zircon Inheritance Reveals Exceptionally Fast Crustal Magma Generation Processes in Central Iberia during the Cambro-Ordovician. J. Petrol. 48, 2327–2339. https://doi.org/10.1093/petrology/egm061

Belousova, E., Griffin, W., O'Reilly, S.Y., Fisher, N., 2002. Igneous zircon: trace element composition as an indicator of source rock type. Contrib. to Mineral. Petrol. 143, 602–622. https://doi.org/10.1007/s00410-002-0364-7

Belousova, E.A., Griffin, W.L., O'Reilly, S.Y., 2006. Zircon crystal morphology, trace element signatures and Hf isotope composition as a tool for petrogenetic modelling: Examples from Eastern Australian granitoids. J. Petrol. 47, 329–353. https://doi.org/10.1093/petrology/egi077

Brown, M., 2013. Granite: From genesis to emplacement. Bull. Geol. Soc. Am. 125, 1079–1113. https://doi.org/10.1130/B30877.1

Brown, M., 2001. Orogeny, migmatites and leucogranite: A review. Proc. Indian Acad. Sci. Earth Planet. Sci. 110, 313–336. https://doi.org/10.1007/BF02702898

Catlos, E.J., 2013. Versatile Monazite: resolving geological records and solving challenges in materials science: Generalizations about monazite: Implications for geochronologic studies. Am. Mineral. 98, 819–832. https://doi.org/10.2138/am.2013.4336

Chapman, J.B., Gehrels, G.E., Ducea, M.N., Giesler, N., Pullen, A., 2016. A new method for estimating parent rock trace element concentrations from zircon. Chem. Geol. 439, 59–70. https://doi.org/10.1016/j.chemgeo.2016.06.014

Cherniak, D.J., Hanchar, J.M., Watson, E.B., 1997. Rare-earth diffusion in zircon. Chem. Geol. 134, 289–301. https://doi.org/10.1016/S0009-2541(96)00098-8

Claiborne, L.L., Miller, C.F., Walker, B.A., Wooden, J.L., Mazdab, F.K., Bea, F., 2006. Tracking magmatic processes through Zr/Hf ratios in rocks and Hf and Ti zoning in zircons: An example from the Spirit Mountain batholith, Nevada. Mineral. Mag. 70, 517–543. https://doi.org/10.1180/0026461067050348

Clark, C., Fitzsimons, I.C.W., Healy, D., Harley, S.L., 2011. How Does the Continental Crust Get Really Hot? Elements 7, 235–240. https://doi.org/10.2113/gselements.7.4.235

Corfu, F., 2003. Atlas of Zircon Textures. Rev. Mineral. Geochemistry 53, 469–500. https://doi.org/10.2113/0530469

Dini, A., Rocchi, S., Westerman, D.S., 2004. Reaction microtextures of REE–Y–Th–U accessory minerals in the Monte Capanne pluton (Elba Island, Italy): a possible indicator of hybridization processes. Lithos 78, 101–118. https://doi.org/10.1016/j.lithos.2004.04.045

Dumond, G., Goncalves, P., Williams, M.L., Jercinovic, M.J., 2015. Monazite as a monitor of melting, garnet growth and feldspar recrystallization in continental lower crust. J. Metamorph. Geol. 33, 735–762. https://doi.org/10.1111/jmg.12150

Engi, M., 2017. Petrochronology Based on REE-Minerals: Monazite, Allanite, Xenotime, Apatite. Rev. Mineral. Geochemistry 83, 365–418. https://doi.org/10.2138/rmg.2017.83.12

Engi, M., Lanari, P., Kohn, M.J., 2017. Significant Ages—An Introduction to Petrochronology. Rev. Mineral. Geochemistry 83, 1–12. https://doi.org/10.2138/rmg.2017.83.1

Faure, G., Mensing, T.M., 2005. Isotopes: principles and applications, 3rd ed. ed. John Wiley & Sons, New Jersey.

Foster, G., Parrish, R.R., 2003. Metamorphic monazite and the generation of P-T-t paths. Geol. Soc. London, Spec. Publ. 220, 25–47. https://doi.org/10.1144/GSL.SP.2003.220.01.02

Fraser, G., Ellis, D., Eggins, S., 1997. Zirconium abundance in granulite-facies minerals, with implications for zircon geochronology in high-grade rocks. Geology 25, 607–610. https://doi.org/10.1130/0091-7613(1997)025<0607:ZAIGFM>2.3.CO;2

Gao, L.-E., Zeng, L., Asimow, P.D., 2017. Contrasting geochemical signatures of fluid-absent versus fluid-fluxed melting of muscovite in metasedimentary sources: The Himalayan leucogranites. Geology 45, 39–42. https://doi.org/10.1130/G38336.1
Hallett, B.W., Spear, F.S., 2015. Monazite, zircon, and garnet growth in migmatitic pelites as a record of metamorphism and partial melting in the East Humboldt Range, Nevada. Am. Mineral. 100, 951–972. https://doi.org/10.2138/am-2015-4839
Hanchar, J.M., Westrenen, W. Van, 2007. Rare Earth Elemehavior in Zircon – Melt Systems. Elements 3, 37–42.
Harley, S.L., Kelly, N.M., 2007. Zircon Tiny but Timely. Elements 3, 13–18. https://doi.org/10.2113/gselements.3.1.13
Harley, S.L., Kelly, N.M., Moller, A., 2007. Zircon Behaviour and the Thermal Histories of Mountain Chains. Elements 3, 25–30. https://doi.org/10.2113/gselements.3.1.25
Hayden, L.A., Watson, E.B., Wark, D.A., 2008. A thermobarometer for sphene (titanite). Contrib. to Mineral. Petrol. 155, 529–540. https://doi.org/10.1007/s00410-007-0256-y
Hermann, J., Rubatto, D., 2003. Relating zircon and monazite domains to garnet growth zones: age and duration of granulite facies metamorphism in the Val Malenco lower crust. J. Metamorph. Geol. 21, 833–852. https://doi.org/10.1046/j.1525-1314.2003.00484.x
Hoskin, P.W.O., Ireland, T.R., 2000. Rare earth element chemistry of zircon and its use as a provenance indicator. Geology 28, 627. https://doi.org/10.1130/0091-7613(2000)28<627:REECOZ>2.0.CO;2
Hoskin, P.W.O., Schaltegger, U., 2003. The Composition of Zircon and Igneous and Metamorphic Petrogenesis. Rev. Mineral. Geochemistry 53, 27–62. https://doi.org/10.2113/0530027
Jackson, S.E., Pearson, N.J., Griffin, W.L., Belousova, E.A., 2004. The application of laser ablation-inductively coupled plasma-mass spectrometry to in situ U–Pb zircon geochronology. Chem. Geol. 211, 47–69. https://doi.org/10.1016/j.chemgeo.2004.06.017
Janasi, V. de A., 1999. Petrogênese de granitos crustais na Nappe de Empurrão Socorro-Guaxupé (SP-MG): uma contribuição da geoquímica elemental e isotópica. Universidade de São Paulo.
Janasi, V. de A., Martins, L., Vlach, S.R.F., 2005. Detailed field work in two outcrops of the Nazare Paulista anatectic granite, SE Brazil. Rev. Bras. Geociencias 35, 99–110.
Jochum, K.P., Nohl, U., Herwig, K., Lammel, E., Stoll, B., Hofmann, A.W., 2005. GeoReM: a new geochemical database for reference materials and isotopic standards. Geostand. Geoanalytical Res. 29, 333–338.
Kaneko, Y., Katayama, I., Yamamoto, H., Misawa, K., Ishikawa, M., Rehman, H.U., Kausar, A.B., Shiraishi, K., 2003. Timing of Himalayan ultrahigh-pressure metamorphism: sinking rate and subduction angle of the Indian continental crust beneath Asia. J. Metamorph. Geol. 21, 589–599. https://doi.org/10.1046/j.1525-1314.2003.00466.x
Karmakar, S., Schenk, V., 2015. Neoproterozoic metamorphic events along the eastern margin of the East Sahara Ghost Craton at Sabaloka and Bayuda, Sudan: Petrology and texturally controlled in-situ monazite dating. Precambrian Res. 269, 217–241. https://doi.org/10.1016/j.precamres.2015.08.018
Kelsey, D.E., Clark, C., Hand, M., 2008. Thermobarometric modelling of zircon and monazite growth in melt-bearing systems: examples using model metapelitic and metapsammitic granulites. J. Metamorph. Geol. 26, 199–212. https://doi.org/10.1111/j.1525-1314.2007.00757.x
Kelsey, D.E., Powell, R., 2011. Progress in linking accessory mineral growth and breakdown to major mineral evolution in metamorphic rocks: A thermodynamic approach in the Na 2O-CaO-K 2O-FeO-MgO-Al 2O 3-SiO 2-H 2O-TiO 2-ZrO 2 system. J. Metamorph. Geol. 29, 151–166. https://doi.org/10.1111/j.1525-1314.2010.00910.x
Kirkland, C.L., Smithies, R.H., Taylor, R.J.M., Evans, N., McDonald, B., 2015. Zircon Th/U ratios in magmatic environs. Lithos 212–215, 397–414. https://doi.org/10.1016/j.lithos.2014.11.021
Kohn, M.J., 2016. Metamorphic chronology—a tool for all ages: Past achievements and future prospects. Am. Mineral. 101, 25–42. https://doi.org/10.2138/am-2016-5146
Kohn, M.J., Corrie, S.L., Markley, C., 2015. The fall and rise of metamorphic zircon. Am. Mineral. 100, 897–908. https://doi.org/10.2138/am-2015-5064
Kohn, M.J., Penniston-Dorland, S.C., 2017. Diffusion: Obstacles and Opportunities in Petrochronology. Rev. Mineral. Geochemistry 83, 103 LP – 152. https://doi.org/10.2138/rmg.2017.83.4
Kriegsman, L.M., Nyström, A.I., 2003. Melt segregation rates in migmatites: review and critique of common approaches. Geol. Soc. London, Spec. Publ. 220, 203–212. https://doi.org/10.1144/GSL.SP.2003.220.01.12
Kylander-Clark, A.R.C., 2017. Petrochronology by Laser-Ablation Inductively Coupled Plasma Mass Spectrometry. Rev. Mineral. Geochemistry 83, 183 LP – 198. https://doi.org/10.2138/rmg.2017.83.6
Martins, L., 2005. Geração e migração de magmas graníticos na crosta continental: estudos de detalhe em granitos e migmatitos da região de Nazaré Paulista (SP). Universidade de São Paulo, São Paulo. https://doi.org/10.11606/T.44.2006.tde-19042007-155618

Martins, L., Vlach, S.R.F., Janasi, V. de A., 2009. Reaction microtextures of monazite: Correlation between chemical and age domains in the Nazaré Paulista migmatite, SE Brazil. Chem. Geol. 261, 271–285. https://doi.org/10.1016/j.chemgeo.2008.09.020
McDonough, W.F., Sun, S. -s., 1995. The composition of the Earth. Chem. Geol. 120, 223–253. https://doi.org/10.1016/0009-2541(94)00140-4
Melo, M.G., Lana, C., Stevens, G., Pedrosa-Soares, A.C., Gerdes, A., Alkmin, L.A., Nalini, H.A., Alkmim, F.F., 2017. Assessing the isotopic evolution of S-type granites of the Carlos Chagas Batholith, SE Brazil: Clues from U–Pb, Hf isotopes, Ti geothermometry and trace element composition of zircon. Lithos 284–285, 730–750. https://doi.org/10.1016/j.lithos.2017.05.025
Mora, C.A.S., Campos Neto, M. da C., Basei, M.A.S., 2014. Syn-collisional lower continental crust anatexis in the Neoproterozoic Socorro-Guaxupé Nappe System, southern Brasília Orogen, Brazil: Constraints from zircon U–Pb dating, Sr–Nd–Hf signatures and whole-rock geochemistry. Precambrian Res. 255, 847–864. https://doi.org/10.1016/j.precamres.2014.10.017
Muller, W., 2000. Isotopic Dating of Strain Fringe Increments: Duration and Rates of Deformation in Shear Zones. Science (80-.). 288, 2195–2198. https://doi.org/10.1126/science.288.5474.2195
Müller, W., 2003. Strengthening the link between geochronology, textures and petrology. Earth Planet. Sci. Lett. 206, 237–251. https://doi.org/10.1016/S0012-821X(02)01007-5
Nardi, L.V.S., Formoso, M.L.L., Müller, I.F., Fontana, E., Jarvis, K., Lamarão, C., 2013. Zircon/rock partition coefficients of REEs, Y, Th, U, Nb, and Ta in granitic rocks: Uses for provenance and mineral exploration purposes. Chem. Geol. 335, 1–7. https://doi.org/10.1016/j.chemgeo.2012.10.043
Pettke, T., Audétat, A., Schaltegger, U., Heinrich, C.A., 2005. Magmatic-to-hydrothermal crystallization in the W–Sn mineralized Mole Granite (NSW, Australia). Chem. Geol. 220, 191–213. https://doi.org/10.1016/j.chemgeo.2005.02.017
Piechocka, A.M., Gregory, C.J., Zi, J.-W., Sheppard, S., Wingate, M.T.D.D., Rasmussen, B., 2017. Monazite trumps zircon: applying SHRIMP U–Pb geochronology to systematically evaluate emplacement ages of leucocratic, low-temperature granites in a complex Precambrian orogen. Contrib. to Mineral. Petrol. 172, 63. https://doi.org/10.1007/s00410-017-1386-5
Pyle, J.M., Spear, F.S., 2003. Four generations of accessory-phase growth in low-pressure migmatites from SW New Hampshire. Am. Mineral. 88, 338–351. https://doi.org/10.2138/am-2003-2-311
Raimondo, T., Payne, J., Wade, B., Lanari, P., Clark, C., Hand, M., 2017. Trace element mapping by LA-ICP-MS: assessing geochemical mobility in garnet. Contrib. to Mineral. Petrol. 172, 17. https://doi.org/10.1007/s00410-017-1339-z
Ramakrishnan, S.S., Gokhale, K.V.G.K., Subbarao, E.C., 1969. Solid Solubility in the system Zircon - Hafnon. Mater. Res. Bull. 4, 323–327.
Rocha, B.C., Moraes, R., Möller, A., Cioffi, C.R., 2018. Magmatic inheritance vs. UHT metamorphism: Zircon petrochronology of granulites and petrogenesis of charnockitic leucosomes of the Socorro–Guaxupé nappe, SE Brazil. Lithos 314–315, 16–39. https://doi.org/10.1016/j.lithos.2018.05.014
Rocha, B.C., Moraes, R., Möller, A., Cioffi, C.R., Jercinovic, M.J., 2017. Timing of anatexis and melt crystallization in the Socorro–Guaxupé Nappe, SE Brazil: Insights from trace element composition of zircon, monazite and garnet coupled to U Pb geochronology. Lithos 277, 337–355. https://doi.org/10.1016/j.lithos.2016.05.020
Rubatto, D., 2017. Zircon: The Metamorphic Mineral. Rev. Mineral. Geochemistry 83, 261–295. https://doi.org/10.2138/rmg.2017.83.9
Rubatto, D., 2002. Zircon trace element geochemistry: partitioning with garnet and the link between U–Pb ages and metamorphism. Chem. Geol. 184, 123–138. https://doi.org/10.1016/S0009-2541(01)00355-2
Rubatto, D., Chakraborty, S., Dasgupta, S., 2013. Timescales of crustal melting in the Higher Himalayan Crystallines (Sikkim, Eastern Himalaya) inferred from trace element-constrained monazite and zircon chronology. Contrib. to Mineral. Petrol. 165, 349–372. https://doi.org/10.1007/s00410-012-0812-y
Rubatto, D., Hermann, J., 2007. Experimental zircon/melt and zircon/garnet trace element partitioning and implications for the geochronology of crustal rocks. Chem. Geol. 241, 38–61. https://doi.org/10.1016/j.chemgeo.2007.01.027
Rubatto, D., Hermann, J., Berger, A., Engi, M., 2009. Protracted fluid-induced melting during Barrovian metamorphism in the Central Alps. Contrib. to Mineral. Petrol. 158, 703–722. https://doi.org/10.1007/s00410-009-0406-5
Rubatto, D., Williams, I.S., Buick, I.S., 2001. Zircon and monazite response to prograde metamorphism in the Reynolds Range, central Australia. Contrib. to Mineral. Petrol. 140, 458–468. https://doi.org/10.1007/PL00007673
Sato, K., Tassinari, C.C.G., Basei, M.A.S., Siga Júnior, O., Onoe, A.T., Souza, M.D. de, 2014. Sensitive High Resolution Ion Microprobe (SHRIMP IIe/MC) of the Institute of Geosciences of the University of São Paulo, Brazil: analytical method and first results. Geol. USP. Série Científica 14, 3–18. https://doi.org/10.5327/Z1519-874X201400030001

Sawyer, E.W., 2010. Migmatites formed by water-fluxed partial melting of a leucogranodiorite protolith: Microstructures in the residual rocks and source of the fluid. Lithos 116, 273–286. https://doi.org/10.1016/j.lithos.2009.07.003
Sawyer, E.W., 2008. Atlas of Migmatites. NRC Research Press and Mineralogical Association of Canada. https://doi.org/10.1139/9780660197876
Schaltegger, U., Davies, J.H.F.L., 2017. Petrochronology of Zircon and Baddeleyite in Igneous Rocks: Reconstructing Magmatic Processes at High Temporal Resolution. Rev. Mineral. Geochemistry 83, 297 LP – 328.
Spear, F.S., 2004. Fast Cooling and Exhumation of the Valhalla Metamorphic Core Complex, Southeastern British Columbia. Int. Geol. Rev. 46, 193–209. https://doi.org/10.2747/0020-6814.46.3.193
Spear, F.S., Pattison, D.R.M., Cheney, J.T., 2016. The metamorphosis of metamorphic petrology, in: The Web of Geological Sciences: Advances, Impacts, and Interactions II. Geological Society of America, pp. 31–74. https://doi.org/10.1130/2016.2523(02)
Spear, F.S., Pyle, J.M., 2010. Theoretical modeling of monazite growth in a low-Ca metapelite. Chem. Geol. 273, 111–119. https://doi.org/10.1016/j.chemgeo.2010.02.016
Spear, F.S., Pyle, J.M., 2002. Apatite, Monazite, and Xenotime in Metamorphic Rocks. Rev. Mineral. Geochemistry 48, 293–335. https://doi.org/10.2138/rmg.2002.48.7
Spencer, C.J., Kirkland, C.L., Taylor, R.J.M., 2016. Strategies towards statistically robust interpretations of in situ U–Pb zircon geochronology. Geosci. Front. 7, 581–589. https://doi.org/10.1016/j.gsf.2015.11.006
Stepanov, A.S., Rubatto, D., Hermann, J., Korsakov, A. V., 2016. Contrasting P-T paths within the Barchi-Kol UHP terrain (Kokchetav Complex): Implications for subduction and exhumation of continental crust. Am. Mineral. 101, 788–807. https://doi.org/10.2138/am-2016-5454
Swain, G., Hand, M., Teasdale, J., Rutherford, L., Clark, C., 2005. Age constraints on terrane-scale shear zones in the Gawler Craton, southern Australia. Precambrian Res. 139, 164–180. https://doi.org/10.1016/j.precamres.2005.06.007
Taylor, R.J.M., Clark, C., Harley, S.L., Kylander-Clark, A.R.C., Hacker, B.R., Kinny, P.D., 2017. Interpreting granulite facies events through rare earth element partitioning arrays. J. Metamorph. Geol. 35, 759–775. https://doi.org/10.1111/jmg.12254
Taylor, R.J.M., Kirkland, C.L., Clark, C., 2016. Accessories after the facts: Constraining the timing, duration and conditions of high-temperature metamorphic processes. Lithos 264, 239–257. https://doi.org/10.1016/j.lithos.2016.09.004
Tedeschi, M., Pedrosa-Soares, A., Dussin, I., Lanari, P., Novo, T., Pinheiro, M.A.P., Lana, C., Peters, D., 2018. Protracted zircon geochronological record of UHT garnet-free granulites in the Southern Brasília orogen (SE Brazil): Petrochronological constraints on magmatism and metamorphism. Precambrian Res. 316, 103–126. https://doi.org/10.1016/j.precamres.2018.07.023
Thompson, A.B., England, P.C., 1984. Pressure-Temperature-Time Paths of Regional Metamorphism II . Their Inference and Interpretation using Mineral Assemblages in Metamorphic Rocks. J. Petrol. 25, 929–955.
Tomkins, H.S., Powell, R., Ellis, D.J., 2007. The pressure dependence of the zirconium-in-rutile thermometer. J. Metamorph. Geol. 25, 703–713. https://doi.org/10.1111/j.1525-1314.2007.00724.x
Townsend, K.., Miller, C.., D'Andrea, J.., Ayers, J.., Harrison, T.., Coath, C.., 2001. Low temperature replacement of monazite in the Ireteba granite, Southern Nevada: geochronological implications. Chem. Geol. 172, 95–112. https://doi.org/10.1016/S0009-2541(00)00238-2
Vance, D., Müller, W., Villa, I.M., 2003. Geochronology: linking the isotopic record with petrology and textures — an introduction. Geol. Soc. London, Spec. Publ. 220, 1–24. https://doi.org/10.1144/GSL.SP.2003.220.01.01
Watson, E.B., Wark, D.A., Thomas, J.B., 2006. Crystallization thermometers for zircon and rutile. Contrib. to Mineral. Petrol. 151, 413–433. https://doi.org/10.1007/s00410-006-0068-5
Weinberg, R.F., Hasalová, P., 2015. Water-fluxed melting of the continental crust: A review. Lithos 212–215, 158–188. https://doi.org/10.1016/j.lithos.2014.08.021
Wendt, I., Carl, C., 1991. The statistical distribution of the mean squared weighted deviation. Chem. Geol. Isot. Geosci. Sect. 86, 275–285. https://doi.org/10.1016/0168-9622(91)90010-T
Westin, A., Campos Neto, M.C., Hawkesworth, C.J., Cawood, P.A., Dhuime, B., Delavault, H., 2016. A paleoproterozoic intra-arc basin associated with a juvenile source in the Southern Brasilia Orogen: Application of U-Pb and Hf-Nd isotopic analyses to provenance studies of complex areas. Precambrian Res. 276, 178–193. https://doi.org/10.1016/j.precamres.2016.02.004
Whitehouse, M.J., 2003. Rare earth elements in zircon: a review of applications and case studies from the Outer Hebridean Lewisian Complex, NW Scotland. Geol. Soc. London, Spec. Publ. 220, 49–64. https://doi.org/10.1144/GSL.SP.2003.220.01.03

Williams, M.L., Jercinovic, M.J., Hetherington, C.J., 2007. Microprobe Monazite Geochronology: Understanding Geologic Processes by Integrating Composition and Chronology. Annu. Rev. Earth Planet. Sci. 35, 137–175. https://doi.org/10.1146/annurev.earth.35.031306.140228

Williams, M.L., Jercinovic, M.J., Mahan, K.H., Dumond, G., 2017. Electron Microprobe Petrochronology. Rev. Mineral. Geochemistry 83, 153–182. https://doi.org/10.2138/rmg.2017.83.5

Yakymchuk, C., 2017. Behaviour of apatite during partial melting of metapelites and consequences for prograde suprasolidus monazite growth. Lithos 274–275, 412–426. https://doi.org/10.1016/j.lithos.2017.01.009

Yakymchuk, C., Brown, M., 2014. Behaviour of zircon and monazite during crustal melting. J. Geol. Soc. London. 171, 465–479. https://doi.org/10.1144/jgs2013-115

Yakymchuk, C., Clark, C., White, R.W., 2017. Phase Relations, Reaction Sequences and Petrochronology. Rev. Mineral. Geochemistry 83, 13–53. https://doi.org/10.2138/rmg.2017.83.2

Yakymchuk, C., Kirkland, C.L., Clark, C., 2018. Th/U ratios in metamorphic zircon. J. Metamorph. Geol. 36, 715–737. https://doi.org/10.1111/jmg.12307

Zhong, S., Feng, C., Seltmann, R., Li, D., Qu, H., 2018. Can magmatic zircon be distinguished from hydrothermal zircon by trace element composition? The effect of mineral inclusions on zircon trace element composition. Lithos 314–315, 646–657. https://doi.org/10.1016/j.lithos.2018.06.029